JOC Article

Energy Transfer in Oligofluorene-C_{60} and C_{60}-Oligofluorene-C_{60} Donor−Acceptor Conjugates

Cornelia van der Pol,[†] Martin R. Bryce,*[,†] Mateusz Wielopolski,[‡] Carmen Atienza-Castellanos,[‡] Dirk M. Guldi,*[,‡] Salvatore Filippone,[§] and Nazario Martín*[,§]

Department of Chemistry, Durham University, Durham DH1 3LE, UK, Departamento de Química Orgánica, Facultad de Ciencias Químicas, Universidad Complutense, E-28040 Madrid, Spain, and Friedrich-Alexander-Universitat Erlangen-Nurnberg, Institute for Physical Chemistry, Egerlandstrausse 3, D-91058 Erlangen, Germany

m.r.bryce@durham.ac.uk; dirk.guldi@chemie.uni-erlangen.de; nazmar@quim.ucm.es

Received April 3, 2007

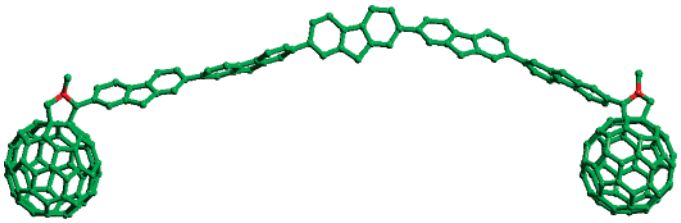

Two complementary series of C_{60}-$(Fl)_n$ and C_{60}-$(Fl)_n$-C_{60} (Fl = 9,9-dihexylfluorene-2,7-diyl; $n = 1-5$) derivatives with terminal *N*-methylfulleropyrrolidine units have been synthesized from CHO-$(Fl)_n$ and CHO-$(Fl)_n$-CHO precursors via 1,3-dipolar cycloaddition reaction of in situ generated azomethine ylides with an excess of C_{60}. In solution electrochemical experiments, these conjugates give rise to amphoteric redox behavior. Three consecutive quasireversible reduction waves have been observed at the expected potentials for the *N*-methylfulleropyrrolidine cores. For the C_{60}-$(Fl)_n$-C_{60} series, each reduction wave is a two-electron process with no observable interaction between the C_{60} units. Two or, in some cases, three oxidation waves—most of them irreversible—are ascribed to the oligofluorene system. These waves are cathodically shifted with an increasing number of fluorene units and anodically shifted by the conjugated terminal aldehyde units, compared to the *N*-methylfulleropyrrolidine termini. Steady-state and time-resolved photolytic techniques show that an efficient transduction of singlet excited-state energy transfer prevails from the photoexcited oligofluorene to the energy accepting fullerene.

Introduction

The advent of fullerenes and their production in multigram quantities at the beginning of the 1990s launched a major effort to explore their outstanding electron acceptor features. Hereby, the delocalization of charges—both electrons and holes—within the spherical carbon framework together with the rigid, confined structure of the aromatic π-sphere offers unique opportunities for stabilizing charged entities. It is, however, the uniquely small reorganization energy that fullerenes exhibit in electron-transfer reactions that renders this carbon allotrope particularly suitable for photovoltaic applications.[1]

An ultimate goal is to design and assemble artificial systems that can efficiently process solar energy, replicating the natural analog. Considering the limited absorption cross-section of C_{60} in the visible range of the solar spectrum, the integration of larger light harvesting arrays is needed to store eventually larger fractions of photonic energy in the charge-separated state.[2] Toward this goal, blends of semiconducting π-conjugated organic polymers, including *p*-phenylenevinylenes (PPVs) and polythiophenes (PTs) with C_{60}, afford new types of plastic solar cells with energy transformation efficiencies that are promising, although the values are comparatively moderate (i.e., relative to silicon-based solar cells). It is crucial to realize that electron-transfer events between the electron-donating polymers and the electron-accepting fullerenes within these composite materials

[†] Durham University.
[‡] Universitat Erlangen-Nurnberg.
[§] Universidad Complutense.

(1) (a) Brabec, C. J.; Sariciftci, N. S.; Hummelen, J. C. *Adv. Funct. Mater.* **2001**, *11*, 15−26. (b) *Energy Harvesting Materials*; Andrews, D. I., Ed.; World Scientific Publishing Co.: Singapore, 2005. (c) Martín, N. *Chem. Commun.* **2006**, 2093−2104.

(2) Winder, C.; Sariciftci, N. S. *J. Mater. Chem.* **2004**, *14*, 1077−1086.

10.1021/jo070686e CCC: $37.00
Published on Web 08/10/2007

evolve with ultrafast dynamics and high quantum efficiencies. However, the tendency of C_{60} to phase separate from the polymer and to crystallize is one of the primary concerns: it imposes unrealistic measures for its solubility in conjugated polymer matrices.[3]

More recently, the "oligomeric" approach[4] has received increasing interest as a result of the breakthroughs in metal-catalyzed cross-coupling synthetic methodologies.[5] Important in this context is that π-conjugated monodispersed oligomers combine the following features: suitable size, electronic and optical properties of the more complex polymer structures, excellent solubility and structure−function relationships. Not surprisingly, systems such as oligo-*p*-phenylenevinylenes (OPVs),[6] oligo-thienylenevinylenes (OTVs),[7] oligo-*p*-phenyleneethynylenes (OPEs),[8] etc., have been used as donor components in a wide range of electron donor−acceptor systems.[6c,9]

On the other hand, oligo- and polyfluorenes are currently receiving considerable attention due to their excellent optical and electronic properties as materials for the preparation of organic light emitting diodes (OLEDs).[10] Recently, low-band gap fluorene copolymers have also been combined with a variety of chemically modified fullerenes to form new plastic solar cells showing power conversion efficiencies as high as 2.2%.[11] However, to the best of our knowledge, fluorene oligomers have not been employed as the electron donor constituent in dyads or triads in the search for photogenerated charge separated states for photovoltaic purposes. In this regard, Wasielewski et al. have recently shown that the length of oligofluorenes (oFls) used as a bridge component between a phenothiazine donor unit and perylene bis(dicarboximide) as an acceptor could be modified without significantly changing the energies of the relevant bridge states; this was a consequence of the charge localization on the two terminal Fl units of the (Fl)$_n$ bridge.[12] This localization provides excellent electronic coupling between the oligomers and the electroactive partner.

CHART 1

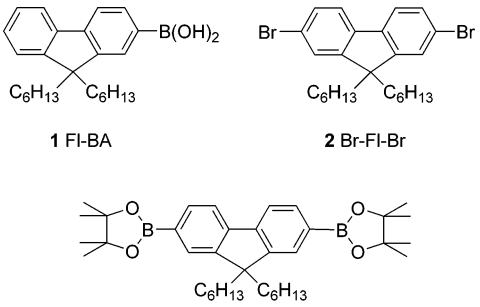

1 Fl-BA **2** Br-Fl-Br

3 BE-Fl-BE

Encouraged by these findings, we have carried out a systematic study of new C_{60}-oligomer dyads and C_{60}-oligomer-C_{60} dumbbell-type triads endowed with oligofluorene moieties of different lengths (i.e., dimer, trimer and pentamer). The present article describes the synthesis, electrochemical study by cyclic voltammetry and the photophysical behavior of these conjugate systems.

Results and Discussion

In the current work, two complementary series of C_{60}-oFl and C_{60}-oFl-C_{60} derivatives have been synthesized by linking one or two fullerene termini, respectively, to functionalized oligofluorenes of different length. First, we have followed a convergent synthetic approach, namely, Suzuki−Miyaura cross coupling reactions[13] between bromine substituted arenes and boronic acids/esters, using fluorene monomers (**1**−**3**)[14] (Chart 1) with two solubilizing hexyl chains to yield the corresponding oligofluorenes.

Next, the oligofluorene building blocks were appended with formyl groups, to enable in the final stage the Prato reaction with C_{60}.[15] Thus, treatment of **2** with butyllithium and DMF in ethyl ether at −78 °C leads to bromofluorene aldehyde **4** in 81% yield (Scheme 1). Formylfluorene boronic ester **5** was

(3) (a) *Fullerenes: From Synthesis to Optoelectronic Properties*; Guldi, D. M., Martín, N., Eds.; Kluwer Academic Publishers: Dordrecht, 2002. (b) Giacalone, F.; Martín, N. *Chem. Rev.* **2006**, *106*, 5136−5190.

(4) (a) *Electronic Materials: The Oligomer Approach*; Müllen, K., Wegner, G., Eds.; Wiley-VCH: Weinheim, 1998. (b) Martin, R. E.; Diederich, F. *Angew. Chem.* **1999**, *111*, 1440−1469; *Angew. Chem., Int. Ed.* **1999**, *38*, 1350−1377. (c) Segura, J. L.; Martín, N. *J. Mater. Chem.* **2000**, *10*, 2403−2435.

(5) *Metal-Catalyzed Cross-Coupling Reactions*; De Meijere, A., Diederich F., Eds.; Wiley-VCH: Weinheim, 1998.

(6) (a) Guldi, D. M.; Luo, C.; Swartz, A.; Gomez, R.; Segura, J. L.; Martín, N.; Brabec C.; Sariciftci, N. *J. Org. Chem.* **2002**, *67*, 1141−1152. (b) Nierengarten, J.-F.; Eckert, J.-F.; Nicoud, J.-F.; Ouali, L.; Krasnikov, V.; Hadziioannou, G. *Chem. Commun.* **1999**, 617−618. (c) Figueira-Duarte, T. M.; Gégout A.; Nierengarten, J.-F. *Chem. Commun.* **2007**, 109−119.

(7) (a) Yamashiro, T.; Aso, Y.; Otsubo, T.; Tang, H.; Harima, Y.; Yamashita, K. *Chem. Lett.* **1999**, 443−444. (b) Hirayama, D.; Yamashiro, T.; Takimiya, K.; Aso, Y.; Otsubo, T.; Norieda, H.; Imahori, H.; Sakata, Y. *Chem. Lett.* **2000**, 570−571. (c) van Hal, P. A.; Knol, J.; Langeveld-Voss, B. M. W.; Meskers, S. C. J.; Hummelen, J. C. Janssen, R. A. J. *J. Phys. Chem. A* **2000**, *104*, 5974−5988. (d) Beckers, E. H. A.; van Hal, P. A.; Dhanabalan, A.; Meskers, S. C. J.; Knol, J.; Hummelen, J. C.; Janssen, R. A. J. *J. Phys. Chem. A* **2003**, *107*, 6218−6224. (e) Ramos, A. M.; Meskers, S. C. J.; van Hal, P. A.; Knol, J.; Hummelen, J. C.; Janssen, R. A. J. *J. Phys. Chem. A* **2003**, *107*, 9269−9283. (f) McClenaghan, N. D.; Grote, Z.; Darriet, K.; Zimine, M.; Williams, R. M.; De Cola, L.; Bassani, D. M. *Org. Lett.* **2005**, *7*, 807−810.

(8) (a) Shirai, Y.; Zhao, Y.; Cheng, L.; Tour, J. M. *Org. Lett.* **2004**, *6*, 2129−2132 (b) Atienza, C.; Insuasty, B.; Seoane, C.; Martín, N.; Ramey, J.; Aminur Rahman, G. M.; Guldi, D. M. *J. Mater. Chem.* **2005**, *15*, 124−132. (c) Atienza, C.; Martín, N.; Wielopolski, M.; Haworth, N.; Clark, T.; Guldi, D. M. *Chem. Commun.* **2006**, *30*, 3202−3204. (d) Clifford, J. N.; Gu, T.; Nierengarten, J.-F.; Armaroli, N. *Photochem. Photobiol. Sci*. **2006**, *5*, 1165−1172.

(9) (a) Segura, J. L.; Martín, N.; Guldi, D. M. *Chem. Soc. Rev.* **2005**, *34*, 31−47. (b) Nierengarten, J. F.; *Solar Energy Mater. Solar Cells* **2004**, *83*, 187−199.

(10) (a) Neher, D. *Macromol. Rapid Commun.* **2001**, *22*, 1365−1385. (b) Scherf, U.; List, E. J. W. *Adv. Mater.* **2002**, *14*, 477−487. (c) Perepichka, I. I.; Perepichka, I. F.; Bryce, M. R.; Pålsson, L.-O. *Chem. Commun*. **2005**, 3397−3399.

(11) (a) Svensson, M.; Zhang, F.; Veenstra, S. C.; Verhees, W. J. H.; Hummelen, J. C.; Kroon, J. M.; Inganäs, O.; Andersson, M. R. *Adv. Mater*. **2003**, *15*, 988−991. (b) Zhang, F.; Perzon, E.; Wang, X.; Mammo, W.; Andersson, M. R.; Inganäs, O. *Adv. Funct. Mater*. **2005**, *15*, 745−750. (c) Wang, X.; Perzon, E.; Oswald, F.; Langa, F.; Admassie, S.; Andersson, M. R.; Inganäs, O. *Adv. Funct. Mater*. **2005**, *15*, 1665−1670. (d) Zhang, F.; Mammo, W.; Andersson, L. M.; Admassie, S.; Andersson, M. R.; Inganäs, O. *Adv. Mater*. **2006**, *18*, 2169−2173.

(12) Goldsmith, R. H.; Sinks, L. E.; Kelley, R. F.; Betzen, L. J.; Liu, W.; Weiss, E. A.; Ratner, M. A.; Wasielewski, M. R. *Proc. Nat. Acad. Sci.* **2005**, *102*, 3540−3545.

(13) (a) Miyaura, N.; Yanagi, T.; Suzuki, A. *Synth. Commun.* **1981**, *11*, 513−519. (b) N. Miyaura, N.; Suzuki, A. *Chem. Rev.* **1995**, *95*, 2457−2483.

(14) (a) Anémian, R.; Mulatier, J.-C.; Andraud, C.; Stéphan, O.; Vial, J.-C. *Chem. Commun.* **2002**, 1608−1609. (b) Kanibolotsky, A. L.; Berridge, R.; Skabara, P. J.; Perepichka, I. F.; Bradley, D. D. C.; Koeberg, M. *J. Am. Chem. Soc.* **2004**, *126*, 13695−13702. (c) Dudek, S. P.; Pouderoijen, M.; Abbel, R.; Schenning, A. P. H. J.; Meijer, E. W. *J. Am. Chem. Soc.* **2005**, *127*, 11763−11768. (d) Hughes, G.; Wang, C.; Batsanov, A. S.; Fearn, M.; Frank, S.; Bryce, M. R.; Perepichka, I. F.; Monkman, A. P. Lyons, B. P. *Org. Biomol. Chem*. **2003**, *1*, 3069−3077.

(15) (a) Prato, M.; Maggini, M. *Acc. Chem. Res.* **1998**, *31*, 519−526. (b) Maggini, M.; Scorrano, G.; Prato, M. *J. Am. Chem. Soc.* **1993**, *115*, 9798−9799.

SCHEME 1

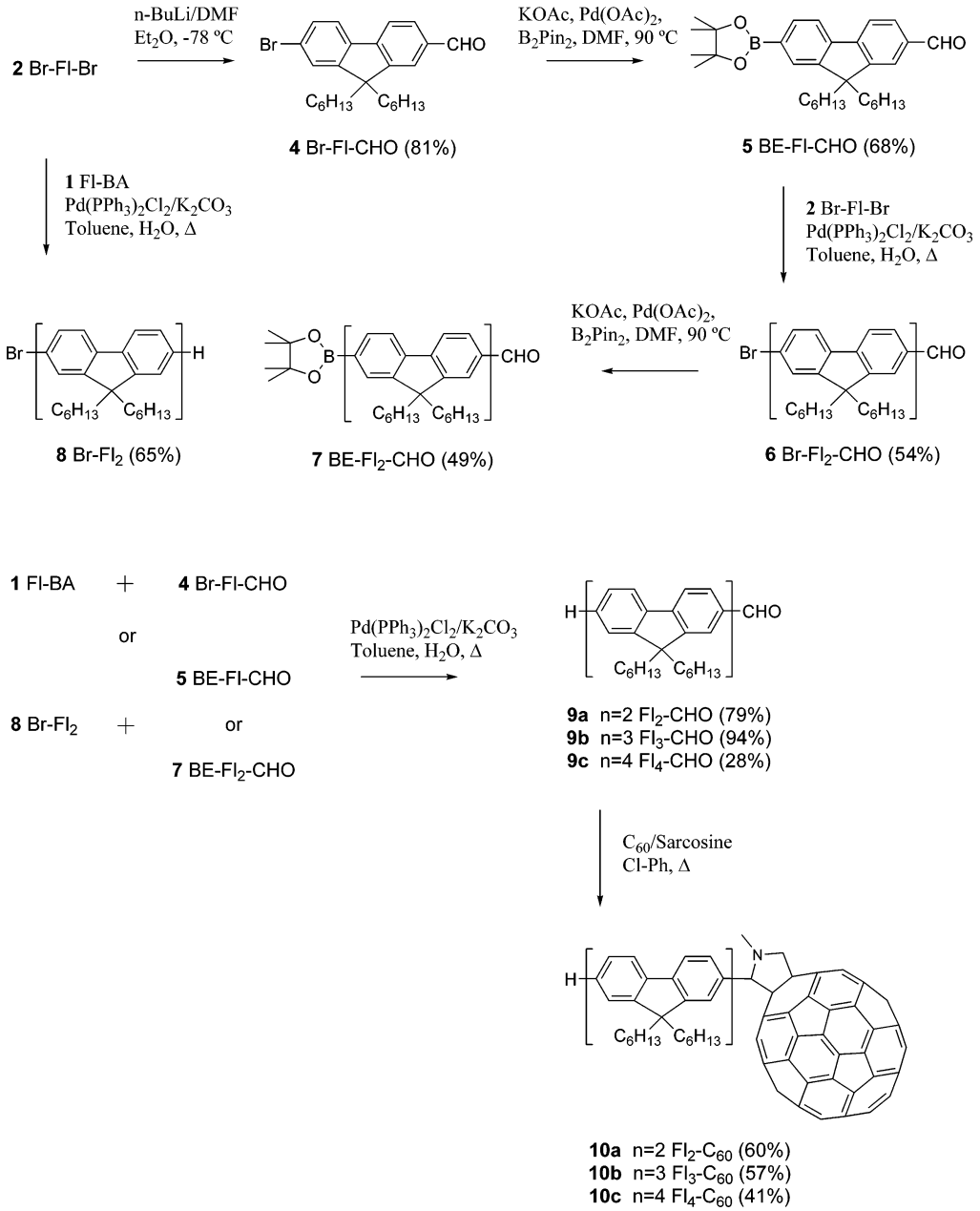

synthesized by heating **4** in DMF at 90 °C with an excess of bis(pinacolato)diboron (B_2Pin_2) in the presence of a catalytic amount of palladium acetate (Scheme 1).

Suzuki reactions were carried out by stirring bromofluorene and fluoreneboronic acid/ester under argon atmosphere in a mixture of H_2O and toluene overnight at 110 °C together with K_2CO_3 and catalytic amounts of $Pd(PPh_3)_2Cl_2$. In the first steps, fluorene dimers **6**, **8**[14b] and **9a** were obtained by reacting **1** with an excess of **2** or **4** and **2** with **5**, respectively, with yields ranging from 54 to 79%. In the same way, the cross-coupling of difluorene bromide **8** with **5** or **7** (which is in turn obtained by replacing the bromine atom in **6** with a boronic ester group) afforded the respective formyl derivatives **9b**,**c**. Cycloadditions to C_{60} of the azomethine ylides, formed *in situ* by reaction of aldehydes **9a**−**c** with sarcosine in refluxing chlorobenzene, led to fulleropyrrolidines **10a**−**c** in moderate yields (Scheme 1).

To obtain the C_{60}-$(Fl)_n$-C_{60} series (**12a**−**c**), the dialdehyde precursors **11a**−**c** were required.

Dimer **11a**, bearing a formyl group at each end, was obtained by direct cross-coupling reaction of formyl bromide **4** with formyl boronic ester **5** in 68% yield (Scheme 2). The trimer and pentamer analogues **11b** and **11c** were obtained from reaction of fluorene diboronic ester **3** with **4** and **6**, respectively, in 59 and 41% yield. Finally, Prato reaction of diformyl oligofluorenes (**11a**−**c**) with sarcosine and an excess of C_{60} afforded dumbbell like compounds **12a**,**b** in good yields; pentameric analog **12c** was obtained in lower yield (Scheme 2).

Electrochemistry. The electrochemical properties of **10a**−**c** and **12a**−**c** were probed by room-temperature cyclic voltammetric measurements in *o*-DCB−CH_3CN solvent mixture (4:1 v/v) with a glassy carbon working electrode, tetrabutylammonium perchlorate, as supporting electrolyte and a scan rate of 100 mV s^{-1}. The redox potentials are collated in Table 1 together with those of **9a**−**c**, **11a**−**c,** pristine [60]fullerene and *N*-methylfulleropyrrolidine (**13**; Chart 2) as references.

SCHEME 2

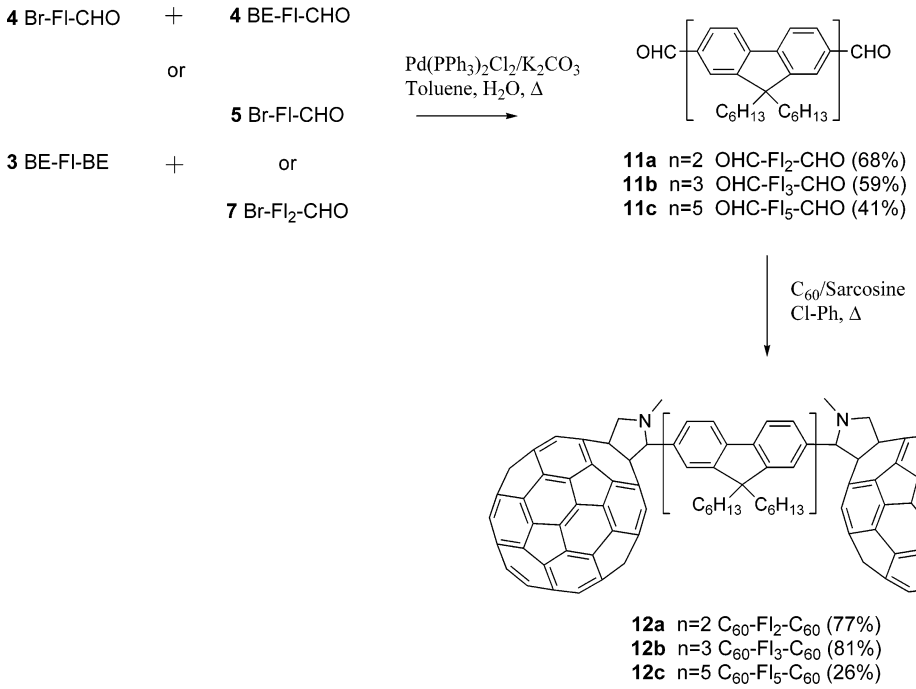

TABLE 1. Redox Potential Values of C_{60} Derivatives 10a−c and 12a−c, Together with Aldehyde Intermediates 9, 11 and Reference Compounds (Pristine C_{60} and 13)[a]

compound	$E^1_{1/2,\,red}$	$E^2_{1/2,\,red}$	$E^3_{1/2,\,red}$	E^4_{red}	E^1_{ox}	E^2_{ox}	E^3_{ox}
C_{60}	−795	−1191	−1649	−2122[b]			
Fl_2-CHO (**9a**)	−2029				1295	1608	1873
Fl_3-CHO (**9b**)	−2080[c]				1114	1332	1800
Fl_4-CHO (**9c**)	−2083[c]				1045	1095	1572
Fl_2-C_{60} (**10a**)	−882	−1293	−1843	−2333	1170	1345	1623
Fl_3-C_{60} (**10b**)	−880	−1292	−1839		1096	1394	1809
Fl_4-C_{60} (**10c**)	−879	−1293	−1848		1032	1195	1555
CHO-Fl_2-CHO (**11a**)	−2102[c]				1411 (1353)[b]	1686	
CHO-Fl_3-CHO (**11b**)	−2058[c]				1179 (1126)[b]	1368[b]	
CHO-Fl_5-CHO (**11c**)	−2078[c]				1087 (1061)[b]	1262[b]	1612
C_{60}-Fl_2-C_{60} (**12a**)	−882	−1294	−1839	−2315	1182	1545	
C_{60}-Fl_3-C_{60} (**12b**)	−884	−1294	−1839	−2344	1123	1473	
C_{60}-Fl_5-C_{60} (**12c**)	−883	−1293	−1838		1125	1477	1641
13	−885	−1280	−1813	−2313	1116	1687	

[a] Potentials in mV; scan rate 100 mVs^{-1}; glassy carbon working electrode, Ag/$AgNO_3$ reference electrode, Pt counter electrode; 0.1 M Bu_4NClO_4 in *o*-DCB/CH_3CN (4:1 v/v). [b] Half wave potential values ($E_{1/2}$). [c] Reduction potential values (E_{red}).

CHART 2

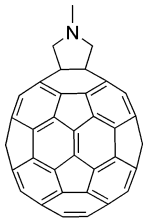

13

As a general feature, **10a−c** and **12a−c** give rise to amphoteric redox behavior. On the reduction side, at least three consecutive one-electron reduction waves—all quasireversible—have been observed. Because a particularly good agreement was found with *N*-methylfulleropyrrolidine **13**, we assign these waves to the reduction steps of the fullerene core (Figure 1). Moreover, they corroborate the lack of electronic communication between the fullerene core and the oligomer moieties in the ground state of **10a−c** and **12a−c**.[6a,8b,16] When contrasting **10a−c** and **12a−c** with pristine [60]fullerene, cathodic shifts to more negative values are observed. This is a clear reflection of saturating a double bond of the C_{60} core as a consequence of the functionalization and raising the LUMO energy in **10a−c** and **12a−c**.[17] The two C_{60} units in **12a−c** act independently: each reduction wave is, therefore, assigned to a two-electron process.

On the oxidation side, derivatives **9**, **10**, **11** and **12** display two or, in some cases, three oxidation waves—most of them irreversible—ascribed to the oligofluorene system (see the Supporting Information). The first oxidation step at ca. 1100 mV is subject to a notable electron withdrawing effect exerted by the aldehyde group(s). This is particularly pronounced in

(16) (a) Giacalone, F.; Segura, J. L.; Martín, N. *J. Org. Chem.* **2002**, *67*, 3529−3532. (b) Guldi, D. M.; Luo, C.; Swartz, A.; Gomez, R.; Segura, J. L.; Martín, N. *J. Phys. Chem. A* **2004**, *108*, 455−467.

(17) Echegoyen, L.; Echegoyen, L. E. *Acc. Chem. Res.* **1998**, *31*, 593−601.

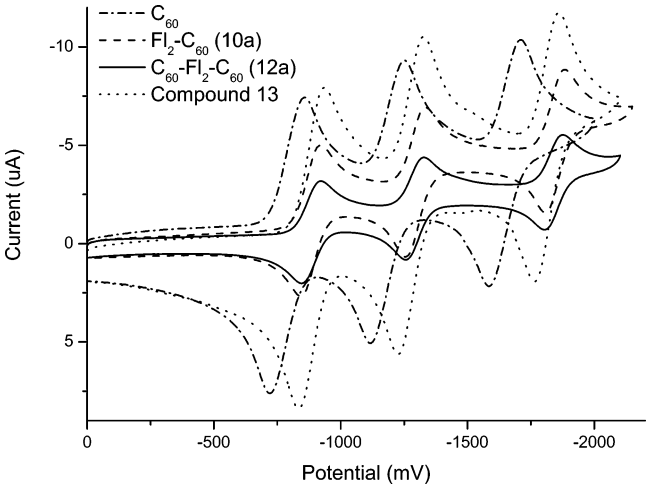

FIGURE 1. Cyclic voltammograms of C_{60}, **10a**, **12a** and **13**. For conditions, see Table 1.

9a (i.e., dimer with one −CHO functionality) and **11a** (i.e., dimer with two −CHO functionalities) with anodic shifts up to 1295 mV and 1411 mV, respectively. Table 1 illustrates that substituting the formyl groups in **9** and **11** by C_{60} shifts the anodic oxidation to less positive values in **10a**−**c** and **12a**−**c**. Implicit here is the loss of conjugation between the electron-withdrawing formyl groups and the oligomer moieties. At the same time, going from the dimer to the trimer and pentamer (**9a** → **9b** → **9c**) sequentially raises the donor character due to a more extended π-conjugation. Consequently, the oxidation values shift cathodically: e.g. E^1_{ox} 1170 mV (**10a**), 1096 mV (**10b**), 1032 mV (**10c**). A similar trend evolves for **11a**−**c** where the first quasireversible waves shift between E^1_{ox} 1411 and 1087 mV (see Table 1). This trend is also observed for **12a** and **12b**, although a further cathodic shift is not seen for **12c**.

Photophysics. First, the steady-state fluorescence spectra of **9a**−**c** and **11a**−**c** were recorded upon 345 nm photoexcitation. In general, all oligofluorenes fluoresce strongly throughout the visible region, Figure 2a, which renders this particular feature extremely valuable to dissect excited-state interactions with C_{60} in **10a**−**c** and **12a**−**c**. Not surprisingly, when inspecting the oligofluorene fluorescence in **10a**−**c** and **12a**−**c** under identical experimental conditions, a marked fluorescence quenching is seen. The quenching, for example, in toluene is as high as 10^3 (i.e., **12a**: 0.30×10^3; **12b**: 1.47×10^3; **12c**: 0.51×10^3), and these values tend be higher for **12a**−**c** than for **10a**−**c**. Nevertheless, it is important that the fluorescence pattern of the oligofluorenes is still preserved, despite the presence of one or two C_{60} units. Turning to the near-infrared region of the fluorescence spectrum, Figure 2b, the observed features resemble those known for **13**.[18] Notably, a 370 nm photoexcitation directs the light nearly quantitatively to the oligofluorenes and not to C_{60}. A reasonable explanation implies transduction of singlet excited-state energy from the oligofluorenes (2.70 eV) to C_{60} (1.76 eV). Independent confirmation for this hypothesis was obtained from excitation spectra, where the fluorescence wavelength was kept constant at 715 nm and the excitation wavelength was systematically varied (not shown). An exceptionally good agreement with the ground state absorption spectrum confirms that the C_{60} fluorescence evolves, largely,

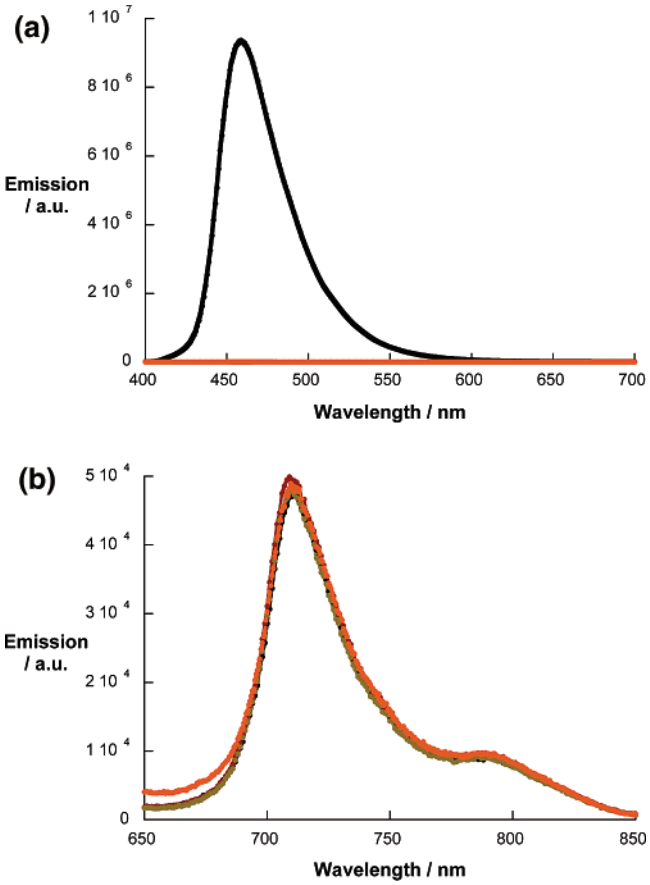

FIGURE 2. (a) Fluorescence spectra of **11a** (black spectrum), **12a** (red spectrum), **12b** (green spectrum) and **12c** (orange spectrum), in THF, with matching absorption of 0.2 at the 345 nm excitation wavelength, (b) Fluorescence spectra of **13** (black spectrum), **12c** (red spectrum), **12a** (green spectrum) and **12b** (orange spectrum) in THF, with matching absorption of 0.2 at the 370 nm excitation wavelength.

from singlet energy transfer and, to a minor extent, from direct excitation. Quantification of the energy transfer reaction was possible through comparing the C_{60} fluorescence quantum yields in solutions of **10a**−**c** and **12a**−**c** in toluene with that of **13** as an internal reference under exactly the same experimental conditions. Quantum yields of nearly 6.0×10^{-4} in all samples speak for a quantitative energy transfer in **10a**−**c** and **12a**−**c**.

In parallel with the steady-state experiments, we probed the fluorescence lifetimes of **10a**−**c** and **12a**−**c** and compared them to the references, namely, oligofluorenes (i.e., **9a**−**c** and **11a**−**c**) and C_{60} (i.e., **13**), which possessed lifetimes of the order of a few ns in the visible and near-infrared regions, respectively. In contrast, **10a**−**c** and **12a**−**c** lack any fluorescence with appreciable lifetimes in the visible range, that is, the oligofluorene part. Only the near-infrared range—the C_{60} part—gave rise to a detectable fluorescence with a lifetime of 1.4 ns. The rise of the C_{60} fluorescence is, however, instantaneous and is masked by the instrumental time resolution of ca. 100 ps, preventing an accurate determination of the energy transfer dynamics.

In the final part of our investigation, the oligofluorenes were tested in femto- (i.e., 387 nm) and nanosecond (i.e., 355 nm) transient absorption measurements, where both constituents are nearly equally photoexcited. First, consider compounds **11a**−**c**. They revealed upon photoexcitation the nearly instantaneous generation (i.e., <0.5 ps, Figure 3a) of metastable singlet excited-state transients (i.e., 0.8 ns, Figure 3b). The spectral

(18) Gialcone, F.; Segura J.; Martín, N.; Ramey, J.; Guldi, D. M. *Chem.*−*Eur. J.* **2005**, *11*, 4819−4834.

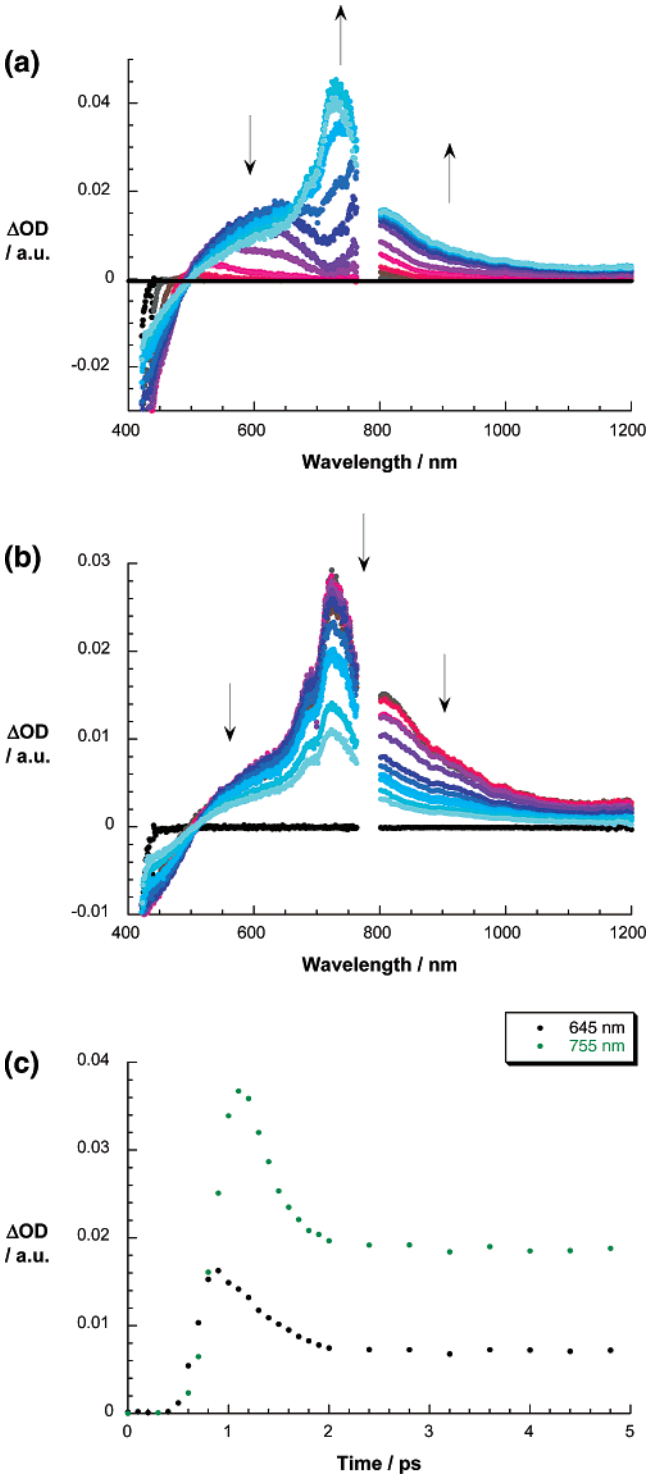

FIGURE 3. (a) Differential absorption spectra (visible and near-infrared) obtained upon femtosecond flash photolysis (387 nm) of **11b** in nitrogen-saturated THF solutions with several time delays between 0 and 20 ps at room temperature. (b) Differential absorption spectra (visible and near-infrared) obtained upon femtosecond flash photolysis (387 nm) of **11b** in nitrogen-saturated THF solutions with several time delays between 0 and 1600 ps at room temperature. (c) Time-absorption profiles of the spectra shown above at 645 and 755 nm, monitoring the formation of the singlet excited state.

characteristics of these transients are ground state bleaching in the 400−450 nm range and new transient absorption in the 600−1200 nm range. The transient maxima vary with the length

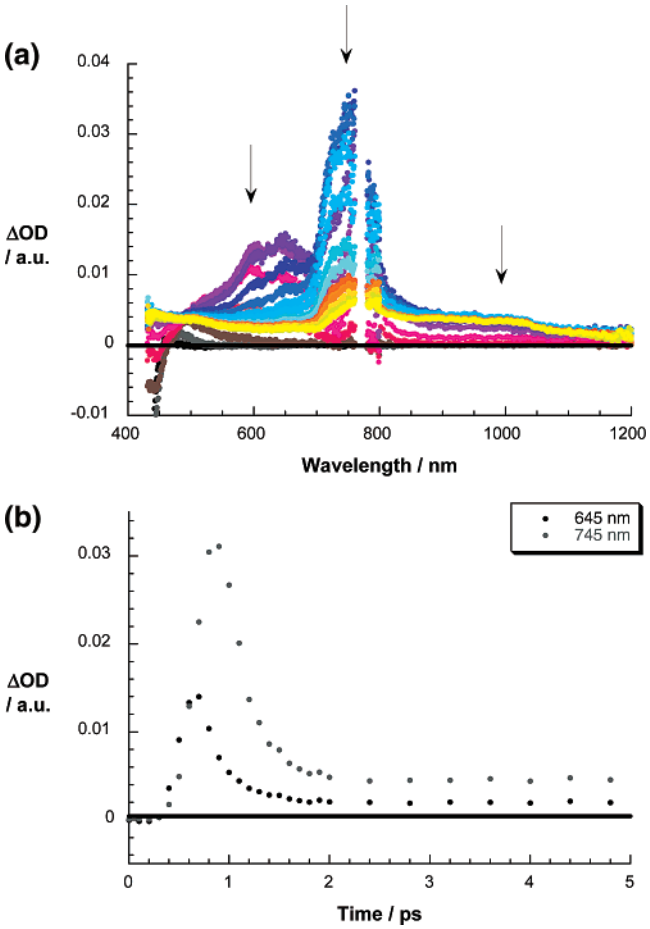

FIGURE 4. (a) Differential absorption spectra (visible and near-infrared) obtained upon femtosecond flash photolysis (387 nm) of **12b** in nitrogen-saturated THF solutions with several time delays between 0 and 2 ps at room temperature. (b) Time-absorption profiles of the spectra shown above at 645 and 745 nm, monitoring the formation of the singlet excited state.

of the oligofluorene unit: 670 nm (dimer, **11a**), 725 nm (trimer, **11b**) and 725 nm (pentamer, **11c**). Interestingly, the exciton appears to be confined in a very short conjugation length. the product of the decay (i.e., 0.8 ns) is the corresponding triplet excited-state of **11a**−**c**.

Initially upon photoexciting **10a**−**c** and **12a**−**c** transient species evolve, which disclose features commonly seen in the oligofluorene references (**11a**−**c**), namely, transient bleach (i.e., below 450 nm) and transient maxima (i.e., around 700 nm), see Figure 4. Such an observation is important, because it attests—in close agreement with the ground state absorption at λ_{exc} 387 nm—the successful excitation of the oligofluorene moieties. However, the oligofluorene singlet excited-state features decay much faster than that observed for the intersystem crossing process in **11a**−**c**. Typical rate constants for this decay are on the order of $\sim 10^{12}$ s^{-1}. Such values confirm the quantitative quenching of the oligofluorene fluorescence in **10a**−**c** and **12a**−**c**. Interestingly, comparing the rate constants of oligofluorene deactivation between the **10a**−**c** series and the **12a**−**c** series a 2-fold acceleration is seen for the latter series (i.e., **10a**: 0.9 ps; **10b**: 1.3 ps; **10c**: 1.9 ps; **12a**: 0.6 ps; **12b**: 0.7 ps; **12c**: 1.0 ps). In other words, placing two C_{60} instead of one C_{60} on the oligofluorene assists in accelerating the excited-state decay. At the conclusion of the oligofluorene decay, only

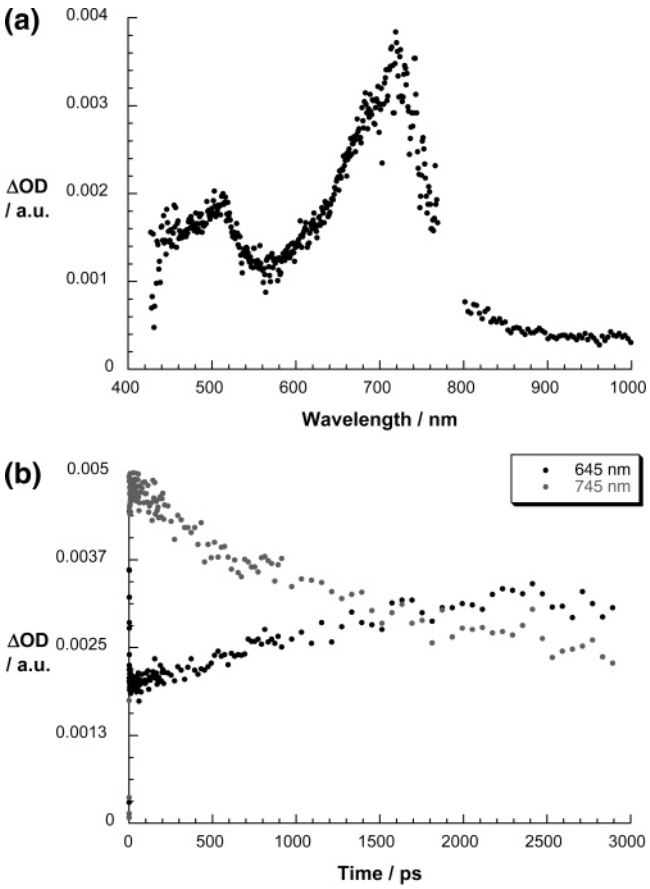

FIGURE 5. (a) Differential absorption spectra (visible and near-infrared) obtained upon femtosecond flash photolysis (387 nm) of **12b** in nitrogen-saturated THF solutions with a time delay of 3000 ps at room temperature, indicating the fullerene triplet−triplet features. (b) Time-absorption profiles of the spectra shown above at 645 and 745 nm, monitoring the decay of the singlet excited-state and formation of the triplet excited state.

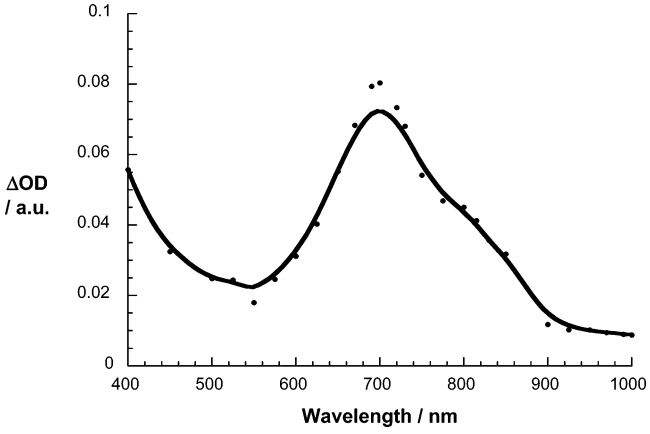

FIGURE 6. Differential absorption spectra (visible and near-infrared) obtained upon femtosecond flash photolysis (355 nm) of **12b** (2.0×10^{-5} M) in nitrogen-saturated THF solutions with a time delay of 100 ns at room temperature, indicating the fullerene triplet−triplet features.

the C_{60} singlet excited-state features are discernible, that is, a transient maximum at 880 nm.

On a time-scale of up to 3.0 ns, the C_{60} singlet excited-state intersystem crosses to the corresponding triplet manifold. Importantly, the kinetics of the singlet decay and the triplet growth match each other reasonably well to yield intersystem crossing rates in **10a**−**c** and **12a**−**c** of 6.5×10^8 s^{-1}, Figure 5b. The most prominent feature of the C_{60} triplet excited-state is a 700 nm maximum as it evolves toward the end of the time-scale of our femtosecond experiments (i.e., 3.0 ns), Figure 5a. In complementary nanosecond experiments with **10a**−**c** and **12a**−**c**, the same triplet transient is seen, which in the absence of molecular oxygen, decays with multiexponential kinetics. An illustration is given in Figure 6.

Conclusions

We have carried out the rational design and synthesis of C_{60}-$(Fl)_n$ derivatives **10a**−**c** and C_{60}-$(Fl)_n$-C_{60} derivatives **12a**−**c** in which 9,9-dihexylfluorene oligomers of well-defined length are attached to *N*-methylfulleropyrrolidine termini. The new compounds were prepared using Suzuki cross-coupling methodology to assemble oligofluorenes with terminal aldehyde units, followed by Prato 1,3-dipolar cycloaddition reactions of *in situ* generated azomethane ylides with C_{60}. The solution electrochemical data show amphoteric behavior (three one-electron reduction waves of each C_{60} core) and irreversible oxidations of the oligofluorene chains with no significant interaction between these electroactive partners in the ground state. Fluorescence time-resolved and steady-state experiments were carried out to determine the photophysical behavior of the new compounds. In particular, an efficient transduction of singlet excited-state energy transfer prevails from the photoexcited oligofluorene to the energy-accepting fullerene. Importantly, no spectral evidence has been found that would suggest a competing electron-transfer reactions that would evolve from the energetically high lying singlet excited states of the oligofluorenes. Future work will address D-$(Fl)_n$-C_{60} ensembles where D is a strong electron donor group designed to further probe the effect of integrating oligofluorene molecular wires into donor−acceptor pairs.

Experimental Section

^{13}C and ^1H NMR spectra were recorded with either a 300, 400 or 500 MHz spectrometer for ^1H NMR and either a 50, 75, 100 or 125 MHz spectrometer for ^{13}C NMR. Chemical shifts are given as δ values (internal standard: TMS). Cyclic voltammograms were recorded on a potentiostat/galvanostat equipped with a software GPES for Windows version 4.8. The electrochemical analyses were carried out using a GCE (glassy carbon) as working electrode, SCE (standard calomel) as reference electrode, Bu_4NClO_4 as supporting electrolyte and *o*-dichlorobenzene/acetonitrile (ratio 4:1 v/v) as solvent at a scan rate of 100 mV/s.

All reactions that required inert or dry atmosphere were carried out under a blanket of argon, which was dried by passage through a column of phosphorus pentoxide. All reagents employed were of standard reagent grade and used as supplied. Dry solvents were obtained from a solvent purification system. Analytical thin layer chromatography (TLC) was performed on silica gel, 60 F_{254} 0.2 mm thickness precoated TLC plates. Column chromatography was carried out using silica (70−230 mesh). Solvents for chromatography were used as supplied.

7-Bromo-9,9-dihexylfluorene-2-carbaldehyde (4). *n*-Butyllithium in hexane (2.5 M, 4.0 mL, 10 mmol) was added dropwise under argon to 2,7-dibromo-9,9-dihexylfluorene **2** (5.2 g, 11 mmol) in dry ether (60 mL) at −78 °C. After stirring at −78 °C for 30 min, the mixture was stirred at room temperature for 30 min. The mixture was cooled to −78 °C and DMF (1.1 mL) was added. The reaction was stirred overnight, while slowly allowed to reach room temperature. HCl (2 M, 50 mL) was added, and the mixture was stirred

for an additional 2 h. The organic layer was separated, and the acid layer was extracted with ether. Both organic layers were combined, and dried over $MgSO_4$, and solvent was removed *in vacuo*. Purification by column chromatography (silica gel eluted by hexane containing a gradient of DCM 0−25%) yielded **4** (3.80 g, 81%) as clear, oily crystals, which in time turned into a white solid. mp: 43−44 °C. ^{1}H NMR (400 MHz, $CDCl_3$): δ 10.06 (1H, s), 7.88−7.85 (2H, m), 7.81 (1H, d, J = 8.0 Hz), 7.64 (1H, d, J = 8.4 Hz), 7.52−7.49 (2H, m), 2.07−1.91 (4H, m), 1.14−0.98 (12H, m), 0.76 (6H, t, J = 7.0 Hz, CH_3), 0.63−0.49 (4H, m). ^{13}C NMR (75 MHz, $CDCl_3$): δ 192.2, 154.2, 151.1, 146.3, 138.5, 135.6, 130.5, 130.4, 126.4, 123.1, 122.2, 120.1, 55.6, 40.1, 31.4, 29.5, 23.7, 22.5, 13.9. HRMS, calcd for $C_{26}H_{33}BrO$ 440.1715; found 440.1714. $C_{26}H_{33}BrO$: calcd C 70.74, H 7.61; found C 70.97, H 7.61.

7-(4,4,5,5-Tetramethyl-1,3,2-dioxaborolan-2-yl)-9,9-dihexylfluorene-2-carbaldehyde (5). Bis(pinacolato)diboron (0.73 g, 2.9 mmol) and 7-bromo-9,9-dihexylfluorene-2-carbaldehyde **4** (0.50 g, 1.2 mmol) were degassed in DMF (10 mL) together with KOAc (0.9 g, 9.2 mmol) for 30 min. A catalytic amount of $Pd(OAc)_2$ (*ca.* 15 mg) was added, and the reaction mixture was stirred overnight at 90 °C under argon. The black precipitate was filtered off, and ethyl acetate (40 mL) was added to the mixture. The organic layer was washed twice with H_2O and dried over $MgSO_4$, and the solvent was evaporated *in vacuo*. Purification by column chromatography (silica gel eluted by hexane containing a gradient of DCM 0−50%) yielded 7-(4,4,5,5-tetramethyl-1,3,2-dioxaborolan-2-yl)-9,9-dihexylfluorene-2-carbaldehyde (**5**) (0.30 g, 68%) as a clear, viscous oil, which in time turned into a white solid. mp: 87−88 °C. ^{1}H NMR (400 MHz, $CDCl_3$): δ 10.06 (1H, s), 7.88−7.85 (4H, m), 7.78 (2H, d, J = 7.6 Hz), 2.06−1.99 (4H, m), 1.40 (12H, s, CH_3), 1.11−0.97 (12H, m), 0.74 (6H, t, J = 7.0 Hz, CH_3), 0.60−0.48 (4H, m). ^{13}C NMR (100 MHz, $CDCl_3$): δ 192.3, 152.1, 151.3, 147.3, 142.4, 135.7, 133.9, 130.3, 129.1, 123.2, 120.4, 120.2, 83.9, 55.4, 40.0, 31.4, 29.5, 24.9, 23.7, 22.5, 13.9. HRMS, calcd for $C_{32}H_{45}BO_3$ 488.3462; found 488.3459. $C_{32}H_{45}BO_3$: calcd C 78.68, H 9.28; found C 78.39, H 9.57.

Br-Fl$_2$-CHO (6). 2,7-Dibromo-9,9-dihexylfluorene (1.2 g, 2.4 mmol, 3.0 equiv, **2**), K_2CO_3 (0.9 g, 6.5 mmol, 8.0 equiv), $Pd(PPh_3)_2Cl_2$ (0.02 g) and 7-(4,4,5,5-tetramethyl-1,3,2-dioxaborolan-2-yl)-9,9-dihexylfluorene-2-carbaldehyde **5** (400 mg, 0.8 mmol) were reacted via Suzuki coupling and purified using hexane with a gradient of DCM (0−100%) as eluent to yield **6** (340 mg, 54%) as a white solid. mp: 124−125 °C. ^{1}H NMR (400 MHz, $CDCl_3$): δ 10.08 (1H, s), 7.91−7.84 (4H, m), 7.76 (1H, d, J = 8.0 Hz), 7.69−7.57 (5H, m), 7.50−7.46 (2H, m), 2.12−1.92 (8H, m), 1.18−0.98 (24H, m), 0.80−0.58 (20H, m). ^{13}C NMR (100 MHz, $CDCl_3$): δ 192.3, 153.3, 153.0, 151.8, 151.2, 147.2, 142.2, 140.5, 139.7, 139.7, 138.8, 135.3, 130.6, 130.1, 126.5, 126.4, 126.3, 123.2, 121.6, 121.5, 121.3, 121.2, 120.1, 120.0, 55.6, 55.5, 40.3, 40.2, 31.4, 29.60, 29.57, 23.80, 23.75, 22.54, 22.51, 13.98, 13.95. HRMS, calcd for $C_{51}H_{65}BrO$ 772.4219; found 772.4221. $C_{51}H_{65}BrO$: calcd C 79.14, H 8.46; found C 79.19, H 8.51.

BE-Fl$_2$-CHO (7). 7-Bromo-9,9,9′,9′-tetrahexyl-2,2′-bifluorenyl-7′-carbaldehyde **6** (0.50 g, 0.7 mmol) and bis(pinacolato)diboron (0.42 g, 1.7 mmol) were degassed in DMF (10 mL) together with KOAc (0.5 g, 5.1 mmol) for 30 min. A catalytic amount of $Pd(OAc)_2$ (*ca.* 15 mg) was added, and the reaction mixture was stirred overnight at 90 °C under argon. The black precipitate was filtered off, and ethyl acetate (40 mL) was added to the mixture. The organic layer was washed twice with H_2O and dried over $MgSO_4$, and the solvent was evaporated *in vacuo*. Purification by column chromatography (silica gel eluted by DCM containing 25% hexane) yielded **7** (260 mg, 49%) as a yellow, viscous oil. ^{1}H NMR (400 MHz, $CDCl_3$): δ 10.08 (1H, s), 7.92−7.58 (12H, m), 2.11−1.99 (8H, m), 1.40 (12H, s), 1.18−0.98 (24H, m), 0.79−0.58 (20H, m). ^{13}C NMR (100 MHz, $CDCl_3$): δ 192.3, 153.0, 152.2, 151.8, 150.2, 147.3, 143.6, 142.4, 140.6, 140.5, 138.7, 135.3, 133.8, 130.6, 129.0, 126.5, 126.2, 123.2, 121.7, 121.6, 121.2, 120.4, 120.0, 119.1, 83.7, 55.4, 55.3, 40.2, 31.4, 29.60, 29.56, 25.0, 23.8, 23.7, 22.52, 22.49, 14.0, 13.9. HRMS calcd for $C_{57}H_{77}BrO_3$ 820.5966; found 820.5967. $C_{57}H_{77}BrO_3 \cdot 1/2H_2O$: calcd C 82.48, H 9.47; found C 82.45, H 9.58.

Fl$_2$-CHO (9a). 7-Bromo-9,9-dihexylfluorene-2-carbaldehyde **4** (184 mg, 0.42 mmol), 9,9-dihexylfluorene-2-boronic acid **1** (150 mg, 40 mmol), K_2CO_3 (392 mg, 2.85 mmol) and $Pd(PPh_3)_2Cl_2$ (40 mg) were reacted via Suzuki coupling. Purification using hexane/DCM (1:1 v/v) as eluent yielded **9a** (220 mg, 79%) as a yellow solid. mp: 55−58 °C. ^{1}H NMR (400 MHz, $CDCl_3$): δ 10.08 (1H, s), 7.91−7.60 (10H, m), 7.39−7.30 (3H, m), 2.11−1.94 (8H, m), 1.15−1.00 (24H, m), 0.79−0.60 (20H, m). ^{13}C NMR (100 MHz, $CDCl_3$): δ 192.4, 152.9, 151.7, 151.5, 151.0, 147.3, 142.4, 140.7, 140.6, 139.9, 138.6, 135.2, 130.6, 127.1, 126.8, 126.5, 126.1, 123.0, 122.9, 121.6, 121.4, 121.2, 120.0, 119.9, 119.8, 55.4, 55.2, 40.3, 40.2, 31.4, 29.7, 29.6, 23.7, 22.54, 22.51, 14.00, 13.97. HRMS, calcd for $C_{51}H_{66}O$ 694.5114; found 694.5111. $C_{51}H_{66}O \cdot H_2O$: calcd C 85.90, H 9.61; found C 86.17, H 9.72.

Fl$_3$-CHO (9b). 7-Bromo-9,9,9′,9′-tetrahexyl-2,2′-bifluorenyl **8** (200 mg, 0.27 mmol), 7-(4,4,5,5-tetramethyl-1,3,2-dioxaborolan-2-yl)-9,9-dihexylfluorene-2-carbaldehyde **5** (130 mg, 0.27 mmol), K_2CO_3 (300 mg, 2.17 mmol) and $Pd(PPh_3)_2Cl_2$ (0.01 g) were reacted via Suzuki coupling and purified using hexane with a gradient of DCM (25−75%) as eluent to yield **9b** (260 mg, 94%) as a yellow viscous oil. ^{1}H NMR (400 MHz, $CDCl_3$): δ 10.08 (1H, s), 7.95−7.59 (16H, m), 7.40−7.28 (3H, m), 2.18−1.97 (12H, m), 1.30−1.00 (36H, m), 0.98−0.60 (30H, m). ^{13}C NMR (100 MHz, $CDCl_3$): δ 192.3, 153.0, 152.0, 151.8, 151.5, 151.0, 147.3, 142.4, 140.8, 140.5, 140.4, 140.0, 139.8, 138.7, 135.3, 130.6, 127.0, 126.8, 126.5, 126.3, 126.2, 126.1, 123.2, 122.9, 121.63, 121.57, 121.5, 121.2, 120.03, 119.98, 119.9, 119.7, 55.43, 55.36, 55.2, 40.4, 40.3, 40.2, 31.5, 31.4, 29.7, 29.63, 29.58, 23.8, 22.54, 22.51, 13.98, 13.95. HRMS, calcd for $C_{76}H_{98}O$ 1026.7618; found 1026.7620. $C_{76}H_{98}O$: calcd C 88.83, H 9.61; found C 88.24, H 9.82.

Fl$_4$-CHO (9c). K_2CO_3 (155 mg, 1.12 mmol, 8.0 equiv), 7-bromo-9,9,9′,9′-tetra-hexyl-2,2′-bifluorenyl **8** (115 mg, 0.15 mmol), 7-(4,4,5,5-tetramethyl-1,3,2-dioxaborolan-2-yl)-9,9,9′,9′-tetrahexyl-2,2′-bifluorenyl-7′-carbaldehyde **7** (115 mg, 0.14 mmol) and $Pd(PPh_3)_2Cl_2$ (0.01 g) were reacted via Suzuki coupling and purified using hexane/DCM (1:1 v/v) as eluent to yield **9c** (53 mg, 28%) as a light-yellow solid containing some impurities (≤5%). Due to the low yield, compound **9c** was used without further purification. ^{1}H NMR (300 MHz, $CDCl_3$): δ 10.12 (1H, s), 7.96−7.59 (22H, m), 7.40−7.28 (3H, m), 2.21−1.97 (16H, m), 1.38−1.00 (48H, m), 0.98−0.60 (40H, m). ^{13}C NMR (75 MHz, $CDCl_3$): δ 192.3, 153.0, 151.9, 151.8, 151.5, 151.0, 147.3, 142.4, 140.8, 140.7, 140.6, 140.49, 140.46, 140.3, 140.1, 140.0, 139.9, 139.8, 138.7, 135.3, 130.6, 128.8, 127.2, 127.0, 136.8, 126.5, 126.2, 126.0, 123.1, 122.9, 121.5, 121.4, 121.2, 120.04, 119.97, 119.9, 119.7, 55.41, 55.36, 55.3, 55.2, 40.4, 40.2, 31.6, 31.4, 29.7, 29.6, 29.4, 23.8, 22.7, 22.6, 22.5, 13.99, 13.96.

Fl$_2$-C_{60} (10a). Sarcosine (36 mg, 0.40 mmol), C_{60} (200 mg, 0.28 mmol) and Fl$_2$-CHO **9a** (48.5 mg, 0.07 mmol) were reacted via the general procedure. Purification using cyclohexane with a gradient of CS_2 (30−100%) as eluent yielded C_{60} (160 mg) and after centrifugation **10a** (60 mg, 60%) as a black solid. ^{1}H NMR (300 MHz, $CDCl_3$): δ 8.10−7.95 (1H, s, br), 7.83−7.47 (9H, m), 7.38−7.29 (3H, m), 5.07 (2H, d, J = 10.0 Hz), 4.35 (1H, d, J = 9.5 Hz), 2.90 (3H, s, NCH_3), 2.32−1.80 (8H, m, br), 0.77 (12H, t, J = 7.0 Hz, CH_3), 1.30−0.12 (32H, m). ^{13}C NMR (75 MHz, $CDCl_3$): δ 156.6, 154.4, 154.10, 154.05, 152.2, 152.1, 151.4, 147.7, 146.8, 146.69, 146.66, 146.59, 146.56, 146.5, 146.4, 145.96, 145.94, 145.80, 145.75, 145.71, 145.66, 145.6, 145.1, 144.83, 144.81, 143.0, 142.7, 142.61, 142.59, 142.51, 142.47, 142.2, 142.1, 141.2, 140.77, 140.75, 140.63, 140.58, 140.3, 127.2, 126.51, 126.45, 123.3, 121.8, 121.7, 120.5, 120.3, 120.1, 84.3, 70.4, 69.5, 55.7, 55.6, 40.8, 40.5, 32.0, 31.9, 30.1, 24.29, 24.25, 24.2, 23.1, 23.0, 14.6, 14.51, 14.46. MALDI-TOF, calcd for $C_{113}H_{71}N$ 1441.6; found *m*/*z* 1443.1 $[M+1]^+$.

Fl_3-C_{60} (10b). C_{60} (175 mg, 0.24 mmol), Fl_3-Al **9b** (62 mg, 0.06 mmol) and sarcosine (25 mg, 0.28 mmol) were reacted via the general procedure. Purification using cyclohexane with a gradient of CS_2 (20−100%) as eluent yielded C_{60} (140 mg) and after centrifugation **10b** (60 mg, 57%) as a black solid. ^{1}H NMR (300 MHz, $CDCl_3$): δ 8.08−7.98 (1H, s, br), 7.85−7.45 (15H, m), 7.38−7.29 (3H, m), 5.07 (2H, d, J = 8.2 Hz), 4.36 (1H, d, J = 9.5 Hz), 2.91 (3H, s, NCH_3), 2.30−1.95 (12H, m, br), 0.79 (18H, t, J = 6.4 Hz, CH_3), 1.40−0.10 (48H, m). ^{13}C NMR (75 MHz, $CDCl_3$): δ 152.20, 152.16, 152.1, 151.9, 151.4, 147.7, 146.9, 146.74, 146.68, 146.64, 146.58, 146.55, 146.5, 146.4, 146.2, 146.00, 145.95, 145.93, 145.88, 145.8, 145.74, 145.70, 145.66, 145.6, 145.1, 144.82, 144.80, 143.5, 143.4, 143.1, 143.0, 142.7, 142.6, 142.49, 142.47, 142.3, 142.2, 142.1, 141.2, 140.94, 140.87, 140.8, 140.7, 140.62, 140.57, 140.4, 140.3, 139.9, 136.3, 136.2, 127.4, 127.2, 126.5, 126.4, 123.3, 121.9, 121.8, 121.7, 120.5, 120.4, 120.3, 120.1, 84.3, 70.4, 69.4, 55.7, 55.6, 40.8, 40.7, 31.9, 31.8, 30.11, 30.05, 24.22, 24.18, 22.98, 22.96, 14.6, 14.5. MALDI-TOF, calcd for $C_{138}H_{103}N$ 1773.8; found *m*/*z* 1774.8 [M + 1].

Fl_4-C_{60} (10c). C_{60} (100 mg, 0.14 mmol), Fl_4-Al **9c** (47 mg, 0.035 mmol) and sarcosine (20 mg, 0.22 mmol) were reacted via the standard procedure. Purification using cyclohexane with a gradient of CS_2 (50−100%) as eluent yielded C_{60} (89 mg) and after centrifugation **10c** (30 mg, 41%) as a black solid. ^{1}H NMR (300 MHz, CS_2 + $CDCl_3$): δ 8.09−8.00 (1H, s, br), 7.85−7.55 (21H, m), 7.35−7.30 (3H, m), 5.07 (2H, d, J = 9.0 Hz), 4.36 (1H, d, J = 10.1 Hz), 2.91 (3H, s, NCH_3), 2.31−1.97 (16H, m, br), 0.81 (24H, t, J = 6.5 Hz, CH_3), 1.45−0.15 (64H, m). ^{13}C NMR (75 MHz, CS_2 + $CDCl_3$): δ 152.2, 151.8, 151.4, 147.7, 147.2, 146.9, 146.8, 146.72, 146.67, 146.61, 146.57, 146.56, 146.4, 146.2, 146.1, 145.97, 145.95, 145.83, 145.75, 145.71, 145.68, 145.6, 145.1, 144.9, 144.8, 143.6, 143.4, 143.1, 143.0, 142.7, 142.6, 142.5, 142.4, 142.2, 142.1, 142.0, 141.3, 141.2, 141.0, 140.9, 140.8, 140.73, 140.65, 140.6, 140.5, 140.43, 140.37, 140.3, 139.9, 137.2, 136.3, 136.2, 127.4, 127.2, 126.6, 126.5, 123.3, 121. 9, 121.8, 121.7, 120.6, 120.43, 120.35, 120.2, 84.3, 70.4, 69.3, 55.7, 55.6, 40.9, 40.5, 32.3, 32.1, 32.0, 30.2, 24.4, 24.3, 23.1, 14.7, 14.5. MALDI-TOF, calcd for $C_{163}H_{135}N$ 2106.1; found *m*/*z* 2107.9 [M + 1], 1387.6, 1302.4.

CHO-Fl_2-CHO (11a). 7-Bromo-9,9-dihexylfluorene-2-carbaldehyde **4** (350 mg, 0.79 mmol), K_2CO_3 (830 mg, 6.01 mmol), 7-(4,4,5,5-tetramethyl-1,3,2-dioxaborolan-2-yl)-9,9-dihexylfluorene-2-carbaldehyde **5** (370 mg, 0.76 mmol) and 0.01 g $Pd(PPh_3)_2Cl_2$ (0.01 g) were reacted via standard Suzuki coupling. Purification using a gradient of hexane/DCM (1:1v/v) to 100% DCM as eluent yielded **13a** (370 mg, 68%) as a pale-yellow solid. mp: 126−127 °C. ^{1}H NMR (400 MHz, $CDCl_3$): δ 10.09 (2H, s), 7.93−7.81 (8H, m), 7.70 (2H, dd, J = 1.6 and 8.0 Hz), 7.65 (2H, d, J = 1.2 Hz), 2.13−2.04 (8H, m), 1.15−0.99 (24H, m), 0.76 (12 H, t, J = 7.0 Hz, CH_3), 0.79−0.59 (8H, m). ^{13}C NMR (100 MHz, $CDCl_3$): δ 192.3, 153.1, 151.8, 147.1, 141.9, 139.1, 135.4, 130.6, 126,6, 123.2, 121.7, 121.3, 120.1, 55.5, 40.2, 31.4, 29.5, 23.8, 22.5, 13.9. HRMS, calcd for $C_{52}H_{66}O_2$ 722.5063; found 722.5070. $C_{52}H_{66}O_2$: calcd C 86.37, H 9.20; found C 86.52, H 9.34.

CHO-Fl_3-CHO (11b). 7-Bromo-9,9-dihexylfluorene-2-carbaldehyde **4** (140 mg, 0.32 mmol), K_2CO_3 (140 mg, 1.01 mmol), 2,7-bis(4,4,5,5-tetramethyl-1,3,2-dioxaborolan-2-yl)-9,9-dihexylfluorene **3** (75 mg, 0.13 mmol) and $Pd(PPh_3)_2Cl_2$ (0.01 g) were reacted via standard Suzuki coupling. Purification used petroleum ether 40:60 with 10% ethyl acetate as eluent to yielded **11b** (80 mg, 59%) as a yellow solid. mp: 65−67 °C. ^{1}H NMR (400 MHz, $CDCl_3$): δ 10.09 (2H, s), 7.93−7.82 (10H, m), 7.75−7.62 (8H, m), 2.15−2.03 (12H, m), 1.18−1.01 (36H, m), 0.93−0.62 (30H, m). ^{13}C NMR (100 MHz, $CDCl_3$): δ 192.3, 153.0, 151.9, 151.8, 147.3, 142.3, 140.3, 140.2, 138.7, 135.3, 130.6, 126.5, 126.3, 123.2, 121.63, 121.60, 121.2, 120.1, 120.0, 55.4, 40.3, 40.2, 31.43, 31.41, 29.60, 29.57, 23.8, 22.5, 13.96, 13.93. HRMS, calcd for $C_{77}H_{98}O_2$ 1054.7567; found 1054.7566. $C_{77}H_{98}O_2$: calcd C 87.61, H 9.36; found C 86.97, H 9.39.

CHO-Fl_5-CHO (11c). 7-Bromo-9,9,9′,9′-tetrahexyl-2,2′-bifluorenyl-7′-carbaldehyde **6** (250 mg, 0.32 mmol), K_2CO_3 (140 mg, 1.01 mmol), 2,7-bis(4,4,5,5-tetramethyl-1,3,2-dioxaborolan-2-yl)-9,9-dihexylfluorene **3** (75 mg, 0.13 mmol) and $Pd(PPh_3)_2Cl_2$ (0.01 g) were reacted via standard Suzuki coupling. Purification used petroleum ether 40:60 with 10% ethyl acetate as eluent to yield **11c** (90 mg, 41%) as a light-yellow, viscous oil. ^{1}H NMR (400 MHz, $CDCl_3$): δ 10.08 (2H, s), 7.93−7.56 (26H, m), 7.50−7.25 (4H, m), 2.16−1.92 (20H, m), 1.20−0.96 (60H, m), 0.89−0.58 (50H, m). ^{13}C NMR (100 MHz, $CDCl_3$): δ 129.3, 153.3, 153.0, 151.8, 151.2, 147.2, 142.2, 140.6, 139.7, 138.8, 135.4, 130.6, 130.1, 126.5, 126.4, 126.3, 123.2, 121.6, 121.5, 121.3, 121.2, 120.1, 55.6, 55. 5, 40.3, 40.2, 31.4, 31.1, 29.7, 29.60, 29.57, 23.81, 23.75, 22.54, 22.51, 13.98, 13.95. HRMS, calcd for $C_{127}H_{162}O_2$ 1719.2575; found 1719.2660.

C_{60}-Fl_2-C_{60} (12a). C_{60} (775 mg, 1.08 mmol), CHO-Fl_2-CHO **11a** (108 mg, 0.15 mmol) and sarcosine (96 mg, 1.08 mmol) were reacted via the standard procedure. Purification using CS_2 with a gradient of $CHCl_3$ (0−100%) as eluent to yielded C_{60} (620 mg) and after centrifugation **12a** (230 mg, 77%) as a black solid. ^{1}H NMR (300 MHz, CS_2 + $CDCl_3$): δ 8.10−7.90 (2H, s, br), 7.90−7.40 (10H, m), 5.04 (4H, d, J = 9.2 Hz), 4.35 (2H, d, J = 9.6 Hz), 2.90 (6H, s, NCH_3, br), 2.35−1.85 (8H, m, br), 1.30−0.10 (44H, m, br). ^{13}C NMR (75 MHz, CS_2 + $CDCl_3$): δ 156.6, 154.4, 154.0, 153.9, 152.0, 147.7, 147.2, 146.9, 146.8, 146.72, 146.69, 146.64, 146.58, 146.56, 146.4, 146.2, 146.1, 146.01, 145.97, 145.9, 145.8, 145.72, 145.69, 145.6, 145.2, 144.94, 144.87, 144.8, 143.6, 143.5, 143.2, 143.1, 142.7, 142.63, 142.58, 142.5, 142.3, 142.2, 142.0, 141.8, 141.2, 140.72, 140.66, 140.4, 139.9, 137.1, 136.4, 136.3, 136.2, 126.8, 121.7, 120.7, 84.3, 70.5, 69.4, 55.6, 41.4, 40.5, 32.6, 32.5, 30.9, 30.6, 24.7, 24.6, 23.8, 23.6, 15.04, 14.96.

C_{60}-Fl_3-C_{60} (12b). C_{60} (278 mg, 0.39 mmol), CHO-Fl_3-CHO **11b** (47 mg, 0.045 mmol) and sarcosine (37 mg, 0.42 mmol) were reacted via the standard procedure. Purification using CS_2 with a gradient of $CHCl_3$ (0−50%) yielded C_{60} (220 mg) and after centrifugation **12b** (92 mg, 81%) as a black solid. ^{1}H NMR (300 MHz, $CDCl_3$): δ 8.14−7.92 (2H, s, br), 7.92−7.40 (16H, m), 5.07 (4H, d, J = 9.6 Hz), 4.36 (2H, d, J = 8.0 Hz), 2.92 (6H, s, NCH_3, br), 2.35−1.80 (12H, m, br), 0.79 (18H, t, J = 6.4 Hz, CH_3), 1.35−0.10 (48H, m, br). ^{13}C NMR (75 MHz, $CDCl_3$): δ 156.6, 154.4, 154.0, 153.9, 152.1, 152.0, 147.7, 147.3, 147.0, 146.8, 146.72, 146.69, 146.63, 146.58, 146.56, 146.4, 146.2, 146.1, 146.0, 145.92, 145.86, 145.8, 145.73, 145.69, 145.66, 145.6, 145.2, 144.93, 144.87, 144.8, 143.6, 143.5, 143.2, 143.1, 142.74, 142.65, 142.62, 142.57, 142.5, 142.4, 142.21, 142.17, 142.0, 141.8, 141.2, 140.9, 140.7, 140.6, 140.4, 140.3, 139.9, 137.1, 136.4, 136.3, 136.1, 126.7, 121.8, 121.7, 120.6, 120.5, 84.3, 70.5, 69.5, 55.7, 41.2, 41.1, 40.5, 32.4, 32.3, 32.2, 30.4, 24.5, 23.6, 23.4, 23.3, 14.84, 14.75, 14.7.

C_{60}-Fl_5-C_{60} (12c). C_{60} (200 mg, 0.28 mmol), CHO-Fl_5-CHO **11c** (60 mg, 0.035 mmol) and sarcosine (25 mg, 0.28 mmol) were reacted via the standard procedure. Purification using CS_2 with a gradient of $CHCl_3$ (0−100%) as eluent yielded C_{60} (160 mg) and after centrifugation **12c** (29 mg, 26%) as a black solid. ^{1}H NMR (300 MHz, $CDCl_3$): δ 8.10−7.90 (2H, s, br), 7.90−7.40 (28H, m), 5.05 (4H, d, J = 7.8 Hz), 4.34 (2H, d, J = 9.5 Hz), 2.90 (6H, s, NCH_3, br), 2.35−1.90 (20H, m, br), 0.78 (30H, t, J = 6.8 Hz, CH_3), 1.30−0.10 (80H, m, br). ^{13}C NMR (75 MHz, $CDCl_3$): δ 154.4, 153.9, 153.6, 152.1, 151.5, 147.7, 147.2, 146.9, 146.74, 146.68, 146.64, 146.58, 146.55, 146.5, 146.4, 146.2, 145.99, 145.95, 145.92, 145.87, 145.8, 145.74, 145.70, 145.65, 145.6, 145.1, 144.82, 144.79, 143.5, 143.4, 143.1, 143.0, 142.7, 142.6, 142.49, 142.46, 142.3, 142.2, 142.0, 141.7, 141.3, 140.61, 140.57, 140.5, 140.3, 140.2, 139.8, 139.6, 137.0, 136.3, 136.2, 130.4, 126.7, 126.6, 126.5, 121.8, 121.7, 121.5, 121.4, 120.5, 120.4, 84.3, 70.4, 69.4, 55.9, 55.7, 40.9, 40.7, 40.5, 32.0, 31.8, 30.1, 30.0, 24.2, 24.1, 23.2, 23.02, 22.97, 14.6, 14.5, 14.4.

Acknowledgment. We thank SFB 583, DFG (GU 517/4-1), FCI and the Office of Basic Energy Sciences of the U.S. Department of Energy, and the ESF Eurocores SONS Programme for funding this work, EPSRC for funding the work at Durham University, and Comunidad de Madrid (Project P-PPQ-000225-0505) and MEC (CTQ-2005-02609).

Supporting Information Available: General procedures for Suzuki−Miyaura cross-couplings and 1,3-dipolar cycloaddition reactions. Copies of ^1H and ^{13}C NMR spectra and additional cyclic voltammograms. This material is available free of charge via the Internet at http://pubs.acs.org.

JO070686E